# A principled (and practical) test for network comparison

**Gecia Bravo-Hermsdorff**                    GECIA@GOOGLE.COM
*Google Research*
*76 9th Ave, New York, NY 10011*


**Lee M. Gunderson**                    LEEG@PRINCETON.EDU
*Gatsby Computational Neuroscience Unit*
*University College London*
*London, W1T 4JG, United Kingdom*


**Pierre-André Maugis**                    PAMAUGIS@GOOGLE.COM
*Google Research*
*Zürich, 8002, Switzerland*


**Carey E. Priebe**                    CEP@JHU.EDU
*Department of Applied Mathematics and Statistics*
*Whiting School of Engineering*
*Johns Hopkins University*
*Baltimore, MD 21218, USA*

## Abstract

How might one test the hypothesis that graphs were sampled from the same distribution? Here, we compare two statistical tests that address this question. The first uses the observed subgraph densities themselves as estimates of those of the underlying distribution. The second test uses a new approach that converts these subgraph densities into estimates of the *graph cumulants* of the distribution. We demonstrate — via theory, simulation, and application to real data — the superior statistical power of using graph cumulants.

**Keywords:** subgraph counts, two-sample test, graph cumulants, network comparison.

## 1. Statement of the problem

In this paper, we use statistics based on subgraph counts to address the following problem:

> Given two samples, $\boldsymbol{G}_A$ and $\boldsymbol{G}_B$, each containing $s$ graphs
> sampled i.i.d. from unknown distributions $\mathcal{G}_A$ and $\mathcal{G}_B$, respectively,
> the goal is to infer whether $\mathcal{G}_A$ and $\mathcal{G}_B$ are different distributions.

## 2. What we are doing (Motivation)

The theory for statistical analysis of i.i.d. data (e.g., the height and weight of different breeds of dogs) is well-established [7, 18]. However, when the data of interest are *interactions* (e.g., who plays with whom in the dog park), a similar consensus has not yet been reached [27].

To analyze such networks of interactions, one common approach is to use statistics based on counts of small substructures (i.e., subgraphs or "motifs") [1, 22, 29, 36]. For example: the densities of "k-star" subgraphs provide increasingly detailed information about a network's degree distribution [32], and the density of cliques of various sizes gives information about the scale of its clustering [28].

To make meaningful comparisons, one must first answer the question: "Compared to what?" The frequently-used clustering coefficient opts to divide the number of "complete" triangles by the number of "incomplete" triangles [25]. The often-cited configuration model compares the observed subgraph counts with those of random networks with the same degree distribution [2, 5].

The recently-proposed graph cumulants offer a natural set of statistics based on a combinatorial view of cumulants (e.g., mean, variance, skew, kurtosis, etc.) [14]. Intuitively, graph cumulants quantify the "excess propensity" of a network for any substructure by systematically comparing the density of that substructure to that which would be "expected" due to the densities of smaller substructures.

Here, we describe a simple statistical test for comparing networks based on graph cumulants. For comparison, we consider the analogous test based on graph moments (i.e., subgraph densities). Our results strongly suggest that graph cumulants should be used as the default statistics in any inferential problem involving subgraph counts.

## 3. What we are not doing (Related work)

There are many ways to compare networks [35]. Here, we describe some other common approaches, highlighting their differences with the setting considered in this paper.

**Spectral methods.** Broadly, these methods use the eigendecomposition of matrices associated with the network, such as the adjacency matrix or the graph Laplacian [8, 24]. Here, we focus instead on statistics based on the frequency of small subgraphs. These two approaches are complementary [19]; flavorfully, spectral methods are more sensitive to the graph's global structure (its "shape"), whereas methods based on subgraph frequencies are more sensitive to the graph's local structure (its "texture").

**Matching nodes.** When the networks being compared have the same set of unique names for all their nodes, it is highly advantageous for statistical tests to incorporate this one-to-one mapping (e.g., when comparing fMRI data of different subjects, it helps to assume that their hippocampi are sufficiently analogous) [10, 11, 34]. However, such information is not always available (e.g., when comparing the social interactions within different schools). This work addresses the latter problem; the nodes are considered to be indistinguishable (i.e., exchangeable), and only the statistics of their pairwise interactions (i.e., their edges) are known to the tests.

**Obtaining significance by sampling.** Many tests for comparing networks require sampling from the inferred distributions to estimate the significance of their differences. Common examples include the use of configuration models [21], exponential random graph models (ERGMs) [3], and geometric random graph models [4]. Such methods are typically computationally intensive, rendering them difficult (or impossible) to implement in practice [12]. The two tests considered in this paper sidestep this issue entirely, analytically computing the significance of the observed differences between the networks.

## 4. How we call things (Notation)

A capital $G$ denotes a single graph with $n$ nodes. All graphs are assumed to be undirected, unweighted, simple graphs.[1]

A calligraphic $\mathcal{G}$ denotes a distribution over such graphs. All graph distributions are assumed to be generated by a single graphon [19] (see Section 7).[2]

A bold $\boldsymbol{G}$ denotes a sample of $s$ graphs from such a distribution. All graphs in a sample are assumed to have the same number of nodes.

A plebeian $g$ denotes a subgraph. An emboldened $\boldsymbol{g}$ denotes a set of subgraphs. The set of subgraphs with at most $r$ edges is denoted by $\boldsymbol{g}_r$ (e.g., $\boldsymbol{g}_3 = \{/, \wedge, //, \triangle, \curlywedge, \sqcap, /\!\!\wedge, /\!\!/\!\!/\}$), and the restriction to connected subgraphs is denoted by $\boldsymbol{g}_r^{(c)}$ (e.g., $\boldsymbol{g}_3^{(c)} = \{/, \wedge, \triangle, \curlywedge, \sqcap\}$). In a few other places (i.e., Section 6), we also use parenthetical superscripts to denote modulations of the variable (never for indices, exponentiation, or derivatives).

---

1. This is for simplicity of presentation; the tests we describe here naturally extend to networks with additional information, such as directed edges, weighted edges, and node attributes [14].
2. Again, this assumption may be relaxed.

The statistics we consider here, namely, graph moments and graph cumulants, have associated with them a particular subgraph $g$ (see Section 5). $\mu_g(\mathcal{G})$ denotes the graph moment (associated with subgraph $g$) of a distribution $\mathcal{G}$ (see Section 5.1), and $\kappa_g(\mathcal{G})$ the corresponding graph cumulant (see Section 5.2). A bold $\boldsymbol{\mu}$ (or $\boldsymbol{\kappa}$) denotes a vector of graph moments (or cumulants), one for each subgraph in $\boldsymbol{g}$.

Estimators of these quantities are given a hat (e.g., $\widehat{\boldsymbol{\mu}}(\boldsymbol{G})$ and $\widehat{\boldsymbol{\kappa}}(\boldsymbol{G})$, see Section 6). Expectation is denoted by angled brackets (e.g., for the unbiased estimators of cumulants $\langle\widehat{\boldsymbol{\kappa}}(\boldsymbol{G})\rangle_{\boldsymbol{G}\sim\mathcal{G}} = \boldsymbol{\kappa}(\mathcal{G})$, see Section 7.1.2).

## 5. Two statistics based on subgraphs (What we measure)

We first define graph moments (Section 5.1), the statistics to which we compare our new method. Then we describe how to convert these to graph cumulants (Section 5.2), the statistics used by our new method.

### 5.1 Graph moments (The typically-used statistics)

When discussing counts of a subgraph $g$ in some larger graph $G$, it is important to distinguish between *induced* counts and *homomorphism* counts [9]; here we are using the latter. Another important distinction is that we are using *injective* homomorphism counts. To obtain these counts, first consider all mappings from the nodes of $g$ to the nodes of $G$.

*Injective* refers to a condition on these node mappings: consider only those mappings that do not send different nodes in $g$ to the same node in $G$.

*Homomorphism* refers to how we decide which of those (injective) mappings are "counts": those for which $G$ has edges at all the locations where there are edges in $g$ (i.e., it is still a count even if there are additional edges in $G$).

The fraction of these mappings that are "counts" are known as injective homomorphism *densities* [19]. These are the graph moments of a graph $G$, denoted by $\mu_g(G)$.

### 5.2 Graph cumulants (The new statistics)

Graph cumulants were recently introduced by Gunderson and Bravo-Hermsdorff [14]. We first review the defining features of cumulants, highlighting a less-well-known combinatorial definition (Section 5.2.1). We then describe the analogue for graphs (Section 5.2.2).
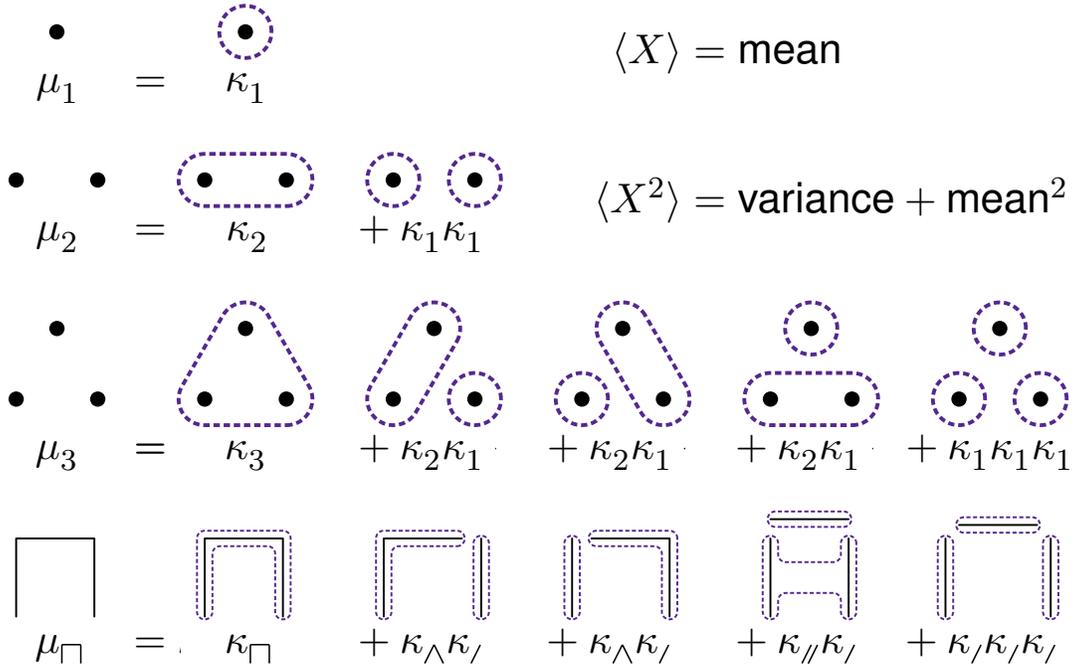
Figure 1: **To expand a graph moment $\mu_g$ in terms of graph cumulants, enumerate all partitions of the edges forming subgraph $g$.**
The top three rows illustrate the combinatorial expansion of the first three classical moments in terms of cumulants (Equation 1). Analogously, the bottom row shows how to expand the graph moment $\mu_\sqcap$ in terms of graph cumulants (Equation 2). The last term ($\kappa_/^3$) corresponds to partitioning this subgraph into three subsets, each with a single edge. The first term ($\kappa_\sqcap$) corresponds to "partitioning" this subgraph into a single subset with all three edges, thus inheriting the connectivity of the entire subgraph. The remaining terms ($\kappa_2\kappa_1$) correspond to partitioning this subgraph into a subset with one edge and a subset with two edges. This can be done in three different ways: in two cases (the two $\kappa_\wedge\kappa_/$ terms), the subset with two edges has those edges sharing a node; and in one case (the $\kappa_{/\!/}\kappa_/$ term), the subset with two edges has those edges not sharing any node.

### 5.2.1 COMBINATORIAL CUMULANTS (BACKGROUND)

First, consider a scalar-valued random variable $X \in \mathbb{R}$ sampled from some distribution $\mathcal{X}$. The $r^{\text{th}}$-order moment of $\mathcal{X}$ is the expectation of the $r^{\text{th}}$ power of $X$: $\mu_r(\mathcal{X}) = \langle X^r \rangle_{X\sim\mathcal{X}}$. These moments may be combined into certain polynomial expressions, known as the cumulants $\kappa_r$ (e.g., mean, variance, skew, kurtosis, etc.).

Cumulants have a uniquely defining property related to sums of independent random variables: the cumulants of the resulting sum are equal to the sum of the cumulants of those

independent random variables [33] (e.g., $\text{Var}(X + Y) = \text{Var}(X) + \text{Var}(Y)$, when $X$ and $Y$ are independent). This is essentially the reason behind the central limit theorem and the ubiquity of the Gaussian distribution [13, 15].

While the classical cumulants are often defined via the cumulant generating function, they also have an equivalent combinatorial definition in terms of a Möbius transform [17, 26] (see Section 12). Namely, the $r^{\text{th}}$ moment can be expressed as a sum of cumulants of order $r$ and lower, corresponding to all partitions of $r$ unique elements (see Figure 1, top three rows). In particular, for our scalar-valued example:

$$\mu_r(\mathcal{X}) = \sum_{\pi \in P_r} \prod_{p \in \pi} \kappa_{|p|}(\mathcal{X}), \tag{1}$$

where $\mu_r$ is the $r^{\text{th}}$ moment, $\kappa_r$ is the $r^{\text{th}}$ cumulant, $P_r$ is the set of all partitions of $r$ unique elements, $\pi$ is one such partition, $p$ is a subset in the partition $\pi$, and $|p|$ is the number of elements in the subset $p$.

Equation 1 may be rearranged to obtain expressions for the cumulants in terms of moments. For example, the third (classical) cumulant (the "skew") is: $\kappa_3 = \mu_3 - 3\mu_2\mu_1 + 2\mu_1^3$. Leveraging this combinatorial definition allows for generalization to random variables with additional structure, such as graphs.

### 5.2.2 Graph cumulants (Definition)

Before describing graph cumulants, it is worth mentioning a subtle point. Notice that Equation 1 relates the moments and cumulants of the *distribution* $\mathcal{X}$ (and not of any finite sample from it $\mathbf{X}$). While this distinction is somewhat pedantic for graph moments (see Section 7.1.1), the combinatorial definition of cumulants (classical or graphical) should only be applied to distributions.

The moments and cumulants of real-valued random variables are indexed by their order $r \in \mathbb{N}$. For graph-valued random variables, moments and cumulants are now indexed by subgraphs $g \in \mathbf{g}$, with order equal to the number of edges in $g$.

In generalizing the combinatorial definition (Equation 1), the partitioning $P_r$ of the edges of the subgraphs must respect their connectivity (see Figure 1, bottom row), i.e.:

$$\mu_g(\mathcal{G}) = \sum_{\pi \in P_{E(g)}} \prod_{p \in \pi} \kappa_{g_p}(\mathcal{G}), \tag{2}$$

where $E(g)$ is the set of edges forming subgraph $g$, $P_{E(g)}$ is the set of partitions of these edges, and $g_p$ is the subgraph formed by the edges in subset $p$.

Again, these may be rearranged to obtain the graph cumulants $\kappa_{\boldsymbol{g}}(\mathcal{G})$ in terms of the graph moments $\mu_{\boldsymbol{g}}(\mathcal{G})$. For example, the ($3^{\text{rd}}$-order) graph cumulant associated with the path

graph with 3 edges is:

$$\kappa_{\sqcap}(\mathcal{G}) = \mu_{\sqcap}(\mathcal{G}) - 2\mu_{\wedge}(\mathcal{G})\mu_{/}(\mathcal{G}) - \mu_{/\!/}(\mathcal{G})\mu_{/}(\mathcal{G}) + 2\mu_{/}^3(\mathcal{G}). \tag{3}$$

## 6. The statistical test (How we compare graphs)

To compare graph moments and graph cumulants on the same footing, we use them as analogous inputs to the same simple statistical test:

1. choose $r$, the maximum order of the graph statistics being considered

2. for each sample, estimate its distribution using these graph statistics

3. quantify the difference between distributions
   using a notion of distance for the space of these graph statistics.

In particular, we consider the graph moments/cumulants associated with $\boldsymbol{g}_r^{(c)}$, the set of connected subgraphs with at most $r$ edges. To measure the difference between two samples of graphs $\mathbf{G}_A$ and $\mathbf{G}_B$, we use the squared Mahalanobis distance [20] between their inferred moments/cumulants:

$$\widehat{d_\mu^2}(\boldsymbol{G}_A, \boldsymbol{G}_B) = \left(\widehat{\boldsymbol{\mu}}_A - \widehat{\boldsymbol{\mu}}_B\right)^\top \left(\widehat{\boldsymbol{\Sigma}}_A^{(\mu)} + \widehat{\boldsymbol{\Sigma}}_B^{(\mu)}\right)^{-1} \left(\widehat{\boldsymbol{\mu}}_A - \widehat{\boldsymbol{\mu}}_B\right), \tag{4}$$

$$\widehat{d_\kappa^2}(\boldsymbol{G}_A, \boldsymbol{G}_B) = \left(\widehat{\boldsymbol{\kappa}}_A - \widehat{\boldsymbol{\kappa}}_B\right)^\top \left(\widehat{\boldsymbol{\Sigma}}_A^{(\kappa)} + \widehat{\boldsymbol{\Sigma}}_B^{(\kappa)}\right)^{-1} \left(\widehat{\boldsymbol{\kappa}}_A - \widehat{\boldsymbol{\kappa}}_B\right). \tag{5}$$

where $\widehat{\boldsymbol{\mu}}_A = \widehat{\boldsymbol{\mu}}(\boldsymbol{G}_A)$ is the vector of estimated moments of sample $\boldsymbol{G}_A$, and $\widehat{\boldsymbol{\Sigma}}_B^{(\kappa)}$ is the covariance estimate of cumulants for sample $\boldsymbol{G}_B$, etc. The next section describes how to compute the estimators used in Equations 4 and 5.

## 7. How to estimate the statistics (What we compute)

In Section 7.1, we describe unbiased estimators for the graph moments and cumulants, high-lighting an important relationship between subgraph densities in the process (Equation 8). In Section 7.2, we build on this idea to describe the typical fluctuations of such sample statistics in terms of their covariance matrices.

### 7.1 Obtaining unbiased estimators (Getting the mean)

We assume that the $s$ observed graphs in a sample $\boldsymbol{G}$ were all obtained by subsampling $n$ nodes i.i.d. from a single (much larger) "graph" $\mathcal{G}$. That is, we assume the model of a single graphon [6, 19]. This assumption allows for several notable simplifications without changing the primary message.

### 7.1.1 For graph moments (Simply plug-in)

Under such node subsampling, graph moments are preserved in expectation, that is:

$$\left\langle \widehat{\mu}_g(\boldsymbol{G}) \right\rangle_{G \sim \mathcal{G}} = \mu_g(\mathcal{G}). \tag{6}$$

Thus, the empirical graph moments $\boldsymbol{\mu}(G)$ are themselves unbiased estimators of the moments of the distribution $\boldsymbol{\mu}(\mathcal{G})$ from which they were sampled. In particular, for a sample of $s$ graphs:

$$\widehat{\mu}_g(\boldsymbol{G}) = \frac{1}{s} \sum_{i=1}^{s} \mu_g(G_i). \tag{7}$$

### 7.1.2 For graph cumulants (Slightly subtle)

To obtain the analogous estimators for graph cumulants, we must be slightly more careful, as products of graph moments are not preserved in expectation under node subsampling. Fortunately, for graphs sampled from the same graphon, products of graph moments are equal to the moment of their disjoint union:

$$\mu_g(\mathcal{G})\mu_{g'}(\mathcal{G}) = \mu_{g \cup g'}(\mathcal{G}). \tag{8}$$

For example, using this relation in the expression for the cumulant associated with the path graph with 3 edges (Equation 3) results in its unbiased estimator:

$$\widehat{\kappa}_{\sqcap}(G) = \mu_{\sqcap}(G) - 2\mu_{/\!\!\wedge}(G) + \mu_{/\!/\!/}(G). \tag{9}$$

In particular, for a sample of $s$ graphs, the estimated cumulants of the underlying distribution are the average of the unbiased estimators of each:

$$\widehat{\kappa}_g(\boldsymbol{G}) = \frac{1}{s} \sum_{i=1}^{s} \widehat{\kappa}_g(G_i). \tag{10}$$

### 7.2 Analytically computing significance (Getting the covariance)

Consider sampling graphs from a distribution $\mathcal{G}$ with known graph moments. The covariance between their observed graph moments is

$$\mathrm{Cov}\big(\mu_g(G), \mu_{g'}(G)\big) = \big\langle \mu_g(G)\mu_{g'}(G) \big\rangle - \big\langle \mu_g(G) \big\rangle \big\langle \mu_{g'}(G) \big\rangle. \tag{11}$$

The last term is trivial; as graph moments are preserved under node subsampling (Equation 6), these expectations are the moments of the distribution itself. The first term, however, is the expectation of a *product* of graph moments. As these are moments of $G$

(a graph with a finite number of nodes), we require a combinatorial modification of Equation 8. Essentially, this involves considering all the ways that these edges could form larger subgraphs [22].[3] The expression is more clearly expressed in terms of subgraph counts, e.g.,

$$c_\wedge(G)c_/(G) = 4c_\wedge(G) + 2c_\triangle(G) + 2c_\lambda(G) + 4c_\sqcap(G) + c_{\text{/\!\!\wedge}}(G). \tag{12}$$

The $4c_\wedge$ term corresponds to the four ways that the two nodes of the edge can be placed to overlap with the wedge ($\wedge$), the $2c_\triangle$ term corresponds to the two ways those nodes can be placed to turn a wedge into a triangle, etc. Converting from counts to moments and taking the expectation allows one to express Equation 11 in terms of moments of the distribution.

As the $s$ graphs in each sample are i.i.d. and have the same number of nodes, the covariance of the sample graph moments is

$$\widehat{\boldsymbol{\Sigma}}^{(\mu)}(\boldsymbol{G}) = \frac{1}{s}\sum_{i=1}^{s}\widehat{\boldsymbol{\Sigma}}^{(\mu)}(G_i). \tag{13}$$

As the unbiased graph cumulants are linear combinations of the sample graph moments, obtaining their covariance follows *mutatis mutandis*:

$$\widehat{\boldsymbol{\Sigma}}^{(\kappa)}(\boldsymbol{G}) = \frac{1}{s}\sum_{i=1}^{s}\widehat{\boldsymbol{\Sigma}}^{(\kappa)}(G_i). \tag{14}$$

## 8. A controlled competition (between the tests)

We first describe the models we use to generate the synthetic data. We then describe how we summarize the quality of the statistical tests, with illustrations for some representative simulations.

### 8.1 Synthetic data (A pair of two-by-two SBMs)

We consider two graph distributions: one with heterogeneous degree distribution (but no community structure), and the other with community structure (but homogeneous degree distribution). Both distributions are stochastic block models (SBMs) [16] with two equal-sized blocks and expected edge density $\rho$.

---

3. This brings up an important point: to obtain the covariance between graph moments/cumulants up to order $r$ (i.e., $\boldsymbol{g}_r$), one must estimate the graph moments/cumulants of the distribution up to order $2r$.

The heterogeneous SBM is parameterized by $\varepsilon_h$, with connectivity matrix:

$$\mathbf{B}_h = \rho \times \begin{bmatrix} 1 + \varepsilon_h & 1 \\ 1 & 1 - \varepsilon_h \end{bmatrix}, \tag{15}$$

where $\varepsilon_h = 0$ gives uniform connection probability between all pairs of nodes, and $\varepsilon_h = 1$ gives zero connection probability within one of the two blocks.

The assortative SBM is parameterized by $\varepsilon_a$, with connectivity matrix:

$$\mathbf{B}_a = \rho \times \begin{bmatrix} 1 + \varepsilon_a & 1 - \varepsilon_a \\ 1 - \varepsilon_a & 1 + \varepsilon_a \end{bmatrix}, \tag{16}$$

where $\varepsilon_a = 0$ again gives uniform connection probability between all pairs of nodes, and $\varepsilon_a = 1$ gives zero connection probability between the two blocks.

After fixing two such SBMs, each instantiation of a two-sample test involves "flipping two coins" to decide which distributions each of the two samples will come from. I.e., the instantiations are split evenly between "different distributions" and "same distribution", with the latter split evenly between the two SBMs.

## 8.2 ROC and AUC curves (How we compare tests)

After computing the squared Mahalanobis distance between a pair of samples (Equations 4 and 5), we use a threshold to classify them as coming from the "same distribution" or "different distributions". Each choice of threshold induces: a rate of false positives (incorrectly concluding that the distributions are different), and a rate of true positives (correctly concluding that the distributions are different). All possible threshold choices are summarized in a Receiver Operating Characteristic (ROC) curve (see Figure 2).

10
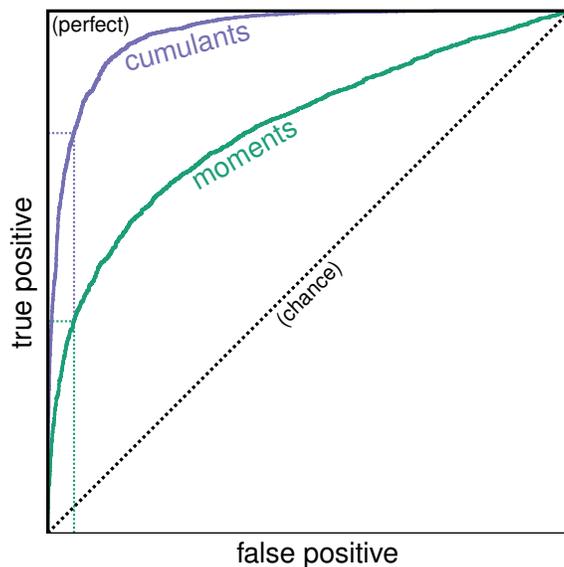
Figure 2: **The statistical power for all possible error rates.**
Known as an ROC curve, this plot visualizes the possible rates of false positives (Type I errors), and false negatives (Type II errors) of a binary classification method. Often, one specifies a maximum rate of false positives, commonly known as $\alpha$. The vertical dotted lines in the lower left illustrate the canonical choice of $\alpha = 0.05$. The point where this vertical line meets the solid curves gives the rate of true positives (i.e., the statistical power, or $1 - $ (Type II error rate)). An ROC curve displays the results for all possible values of $\alpha$: random guesses result in a line along the diagonal, while perfect answers result in a line that hugs the upper left. For this plot, both statistical tests (**moments** and **cumulants**) use the counts of connected subgraphs with up to three edges to distinguish between samples from two graph distributions: a heterogeneous SBM (Equation 15 with $\varepsilon_h = \frac{1}{16}$), and an assortative SBM (Equation 16 with $\varepsilon_a = \frac{1}{16}$), both with density $\rho = \frac{1}{2}$. Each sample contains $s = 4$ graphs, and all graphs have $n = 256$ nodes.

To compare ROC curves, we summarize them with a single scalar value, viz., the Area Under the Curve (AUC). Figure 3 compares the AUC for a range of sample sizes. The use of graph cumulants consistently results in greater statistical power, especially when the number of graphs per sample is small.

One might wonder if these results are sensitive to the model parameters $\varepsilon_h$ and $\varepsilon_a$. While the values used to create the figures were judiciously chosen (e.g., such that the AUC spans the range from chance to perfect), the qualitative conclusions remain robust for (essentially) any parameter choice. In the next section, we show that the use of graph cumulants is similarly promising for applications to more realistic networks.
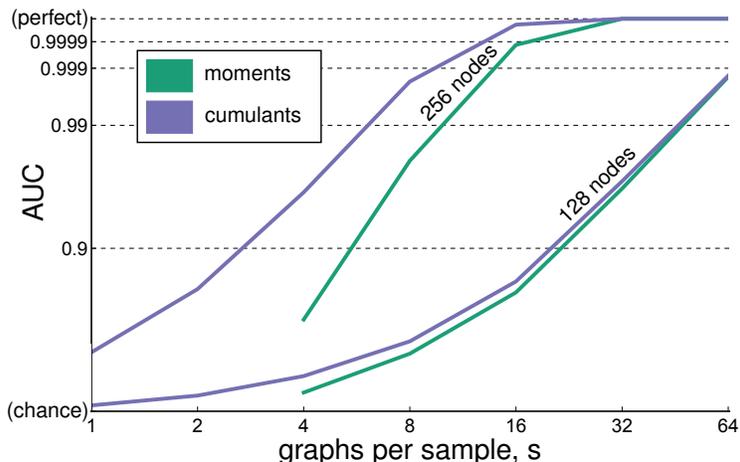
Figure 3: **Using graph cumulants outperforms using graph moments, particularly when the number of graphs per sample is small.**
We construct ROC curves as in Figure 2 for different numbers of graphs per sample $s$, summarizing each by the Area Under its Curve (AUC). (An AUC of $\frac{1}{2}$ corresponds to chance, and 1 to perfect.) Note the $y$-axis has been significantly distorted. The advantage of using graph cumulants is more pronounced for small number of graphs per sample. Indeed, the test using cumulants works even when there is only a *single* observed graph in each sample (see Section 11 and Appendix A), whereas a third-order test using moments fails to give an answer for $s < 4$.

## 9. Studying the tests in the wild (Application to real networks)

As we assume that all graphs in a sample are obtained from a single graphon (Section 7.1), we generate graphs by subsampling a fraction of nodes from several real networks. In particular, we use data from Merid et al. [23] of four genetic interaction networks related to cancer, viz., those of the Mouse, Rat, Human, and Arabidopsis (a small flowering plant related to cabbage and mustard). Figures 4 and 5 show that using graph cumulants to discriminate between these biological networks outperforms the analogous test using graph moments.
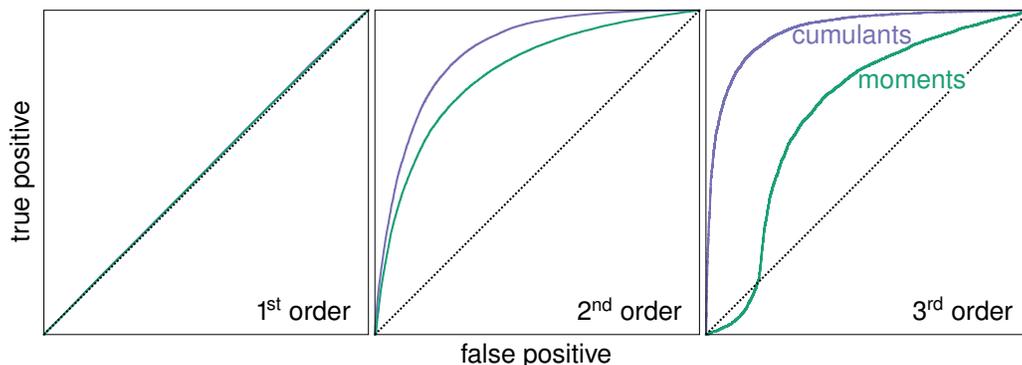
Figure 4: **Increasing the number of subgraphs considered by the model improves statistical power for cumulants, but causes overfitting for moments.**
We use the two tests to compare the genetic interaction networks of Arabidopsis ($\sim 1.3 \times 10^4$ nodes, $\sim 7.9 \times 10^5$ edges) and Mouse ($\sim 1.4 \times 10^4$ nodes, $\sim 9.2 \times 10^5$ edges) (data from [23], adapted such that the networks have same edge density). We use three sets of subgraphs of increasing size, namely, the connected subgraphs containing at most $r = 1$ (*left*), 2 (*middle*), or 3 edges (*right*). To create the ROC curves, we generate samples containing $s = 4$ graphs each. Once a sample was randomly assigned to one of the two original networks, we generate each of its graphs by including each node in the original network i.i.d. with probability such that the expected number of nodes is $n \sim 256$, and taking the resulting induced subgraph.
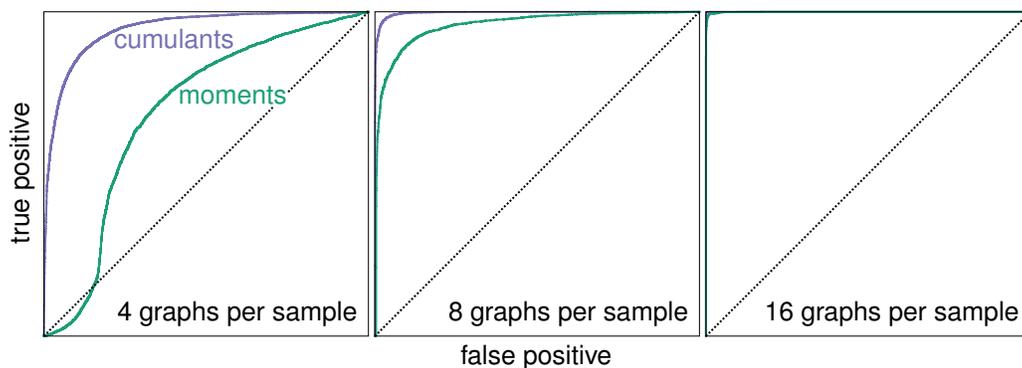


Figure 5: **Cumulants continue to consistently outperform moments in real data, especially when the number of graphs per sample is small.**
We compare the genetic interaction networks of Human ($\sim 1.6 \times 10^4$ nodes, $\sim 13.9 \times 10^5$ edges) and Rat ($\sim 1.1 \times 10^4$ nodes, $\sim 9.0 \times 10^5$ edges). The samples are generated with the same method as in Figure 4. All three plots use connected subgraphs with up to $r = 3$ edges.

13

## 10. Why cumulants do better

Why does using graph cumulants consistently provide better statistical power? After all, unbiased graph cumulants are simply linear combinations of graph moments! (Section 7.1.2) Loosely, the reason is that graph distributions "look more Gaussian" when represented in terms of cumulants (as compared to moments).

Both tests measure differences between distributions using the squared Mahalanobis distance (Equations 4 and 5). As this measure depends only on the mean and covariance, there is a tacit assumption that the sample statistics are well-characterized by a multivariate Gaussian [31].

Indeed, if they *were* exactly Gaussian, and their covariance known exactly, then the squared Mahalanobis distance between pairs of samples from the same distribution would follow a $\chi^2$ distribution. However, as the sample statistics are not precisely Gaussian, and their covariance must be estimated, one expects some deviation from this limiting distribution.

As illustrated in Figure 6, the test using moments results in a distribution of squared Mahalanobis distances with overly-heavy tails. Whereas the distribution for the test using cumulants is well-characterized by the appropriate $\chi^2$ distribution.
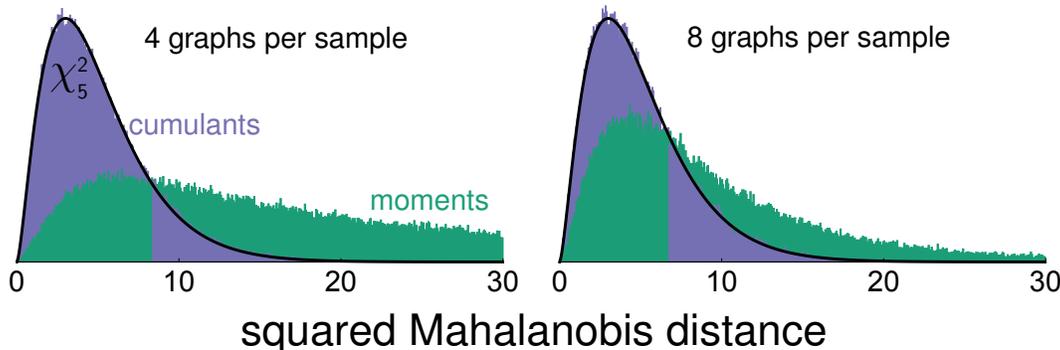


Figure 6: **The test statistic based on graph cumulants remains nearly $\chi^2$, even when only few graphs are observed.**
If a test statistic follows a known distribution under the null hypothesis, one can control the false positive rate by choosing an appropriate threshold. Indeed, for a large number of graphs per sample $s \to \infty$, both tests converge to a $\chi^2$ distribution. As the number of graphs per sample decreases, this becomes a poor approximation for the test using moments. In contrast, the approximation remains strikingly robust for the test using cumulants. Colored histograms are the empirical distributions of the test statistics (Mahalanobis distance squared) for simulations with the same parameters as in Figure 2, and black curves are the limiting $\chi_5^2$ distribution.

## 11. The main message (Discussion)

Perhaps the most salient advantage of using graph cumulants (instead of the subgraph densities themselves) is: the ability to compare distributions even when observing only a *single* graph from each (e.g., Figure 3).

At first glance, it may seem strange that one could make inferences about a distribution from a sample containing only a single "observation". Indeed, this certainly does not work for scalar-valued random variables — a single observation provides no information about the spread of its underlying distribution.

Essentially, this difference arises because, in graphs, the data reside in the edges, but sampling is applied node-wise. Notationally, this manifests itself in our need to specify both $n$ (the number of nodes per graph) and $s$ (the number of graphs per sample), whereas the "quantity" of i.i.d. scalar data is specified by only the sample size.

Thus, there are two relevant limits: we may ask about the distributions of these statistics as either $n$ or $s$ become sufficiently large. As $s \to \infty$, both methods are asymptotically normal. However, as $n \to \infty$ (with $s$ fixed), graph cumulants appear to more properly exploit the multiplicity of the data *within* each graph, allowing for inference even when $s = 1$. In contrast, the test using moments is ill-defined for $s = 1$, or when the number of samples is too small (see Appendix A). Moreover, even in the "classical" limit of $s \to \infty$, the use of graph cumulants remains statistically advantageous (see Appendix B).

In a sense, graph cumulants provide a more "natural" set of coordinates than the subgraph densities themselves. For example, $\kappa_\wedge$ measures the wedge density $\mu_\wedge$ while "taking into account" the lower-order effect of edge density $\mu_/$. In doing so, the second-order graph cumulant $\kappa_\wedge$ becomes "more orthogonal" to the first-order edge density $\mu_/$, in contrast to the strong correlation between $\mu_\wedge$ and $\mu_/$.

Moreover, the covariance estimates for cumulants are more robust, leading to impressively accurate agreement with the classical $\chi^2$ distribution. This allows one to convert these statistics into precise probabilistic statements (e.g.: "What is the likelihood that a single graphon generated both graphs?"). This notion of "graphonic similarity" between any pair of graphs is a remarkably general tool.

## 12. Promising Sequels (Future directions)

As a Coda, we highlight a compelling analogy between the conversion of induced subgraph densities to the homomorphism subgraph densities and the conversion of homomorphism subgraph densities to their corresponding graph cumulants. The former applies a Möbius transform to the poset induced by the inclusion of edges in a subgraph with a fixed number of nodes. The latter also applies a Möbius transform, though with respect to the poset induced by the partitions of an arrangement of a fixed number of edges.

This suggests a general framework for the "cumulantification" of other types of combinatorial objects. Indeed, extensions to hypergraphs and directed networks were described in the Appendices of Gunderson and Bravo-Hermsdorff [14], though the applications appear much more general — any combinatorial structure admitting a similar notion of "subdivision" naturally induces a poset over its substructures, and thus the corresponding cumulants.

## Acknowledgments

## Appendix A. Singular covariance estimates

Below a certain number of observed graphs, the test using moments results in singular covariance matrices. If the sum of the two covariance matrices is also singular, one cannot take its inverse, so the Mahalanobis distance (Equation 4) is ill-defined. Here, we illustrate the simplest example: when there is only $s = 1$ graph per sample, the inferred distributions for the test using moments have zero variance in their edge densities $\mu_{/}$.

Consider a single observed graph $G_1$ with $n$ nodes and $m$ edges. For the test using moments, the expected subgraph densities of the inferred distribution are taken to be those of this observed graph: $\mu_g(\mathcal{G}) = \mu_g(G_1)$. The estimation of the variance of $\mu_{/}$ assumes that the graph moments match to second order (and, as $n$ is fixed, their expected counts as well). At first order, we have

$$\langle c_{/}(G) \rangle_{G \sim \mathcal{G}} = c_{/}(G_1)$$
$$= m. \tag{17}$$

And at second order, we have

$$\langle c_{/}^2(G) \rangle_{G \sim \mathcal{G}} = \langle c_{/}(G) + 2c_{\wedge}(G) + 2c_{/\!/}(G) \rangle_{G \sim \mathcal{G}}$$
$$= c_{/}(G_1) + 2c_{\wedge}(G_1) + 2c_{/\!/}(G_1)$$
$$= m^2. \tag{18}$$

The *only* distributions satisfying both of these constraints are those containing graphs with precisely $m$ edges, and thus the variance in edge density is zero: $\mathrm{Var}(\mu_{/}) = 0$.

In a sense, this can be thought of as a 1×1 covariance matrix of rank 0. In general, as the number of graphs per sample $s$ increases, the rank of the covariance matrix $\mathbf{\Sigma}^{(\mu)}$ does as well. For a given order $r$, one has covariance matrices of size $|\boldsymbol{g}| \times |\boldsymbol{g}|$, and therefore requires sufficiently many graphs per sample $s$ such that the rank of the sum of the two inferred covariance matrices is no less than $|\boldsymbol{g}|$. This is the reason behind the $s < 4$ cutoff for the test using moments in Figure 5.

We remark that, even with sufficient sample size, the covariance matrix may be singular (if a subset of the sample exhibits coincidental colinearity or any of its higher-dimensional analogues). To handle these infrequent cases in a consistent way, we use the *pseudo*inverse in Equations 4 and 5.

## Appendix B. The limit of many observed graphs
## (Asymptotic Relative Efficiency of the two tests)

In Section 10, we show that the test statistic based on graph cumulants follows a $\chi^2$ distribution under the null hypothesis, even when the number of observed graphs $s$ is small, whereas the test statistic based on graph moments does not. However, both statistics indeed do converge to a $\chi^2$ distribution in the limit of many observed graphs $s \to \infty$ [22]. In this section, we compare the statistical power of the two tests in this limit of large sample size, showing that using cumulants still tend to outperform using moments.

To this end, we consider the large sample size limit $s \to \infty$ as the distributions become increasingly similar $\mathcal{G}_1 \to \mathcal{G}_0$. Representing these distributions as SBMs with connection matrices $\mathbf{B}_0$ and $\mathbf{B}_1$, we represent the latter as a perturbation to the former $\mathbf{B}_1 = \mathbf{B}_0 + \sqrt{\gamma/s}\,\delta\mathbf{B}$. The scaling of this perturbation as $s \to \infty$ is such that, given some maximum allowable error rates of false positives $\alpha$ and false negatives $\beta$, there exists a critical value $\gamma_*$ above which these desiderata are achievable.

For two different tests, the ratio of their $\gamma_*$ is known as the Pitman asymptotic relative efficiency (PARE) [30]. As the two tests we are comparing have the same $s \to \infty$ limiting distribution $\chi^2_5$, taking this ratio removes the dependence on $\alpha$ and $\beta$. Thus, the PARE depends on two choices: the distribution $\mathbf{B}_0$ and the perturbation $\delta\mathbf{B}$.

For $\mathbf{B}_0$, we choose a model that allow us to independently control assortativity and heterogeneity. Specifically, we blend the two previously mentioned SBMs (Equations 15 and 16), using the Kronecker product of their connectivity matrices $\mathbf{B}_h$ and $\mathbf{B}_a$, i.e.,

$$\mathbf{B}_0 = \rho \times \begin{bmatrix} (1+\varepsilon_h)(1+\varepsilon_a) & (1+\varepsilon_h)(1-\varepsilon_a) & (1+\varepsilon_a) & (1-\varepsilon_a) \\ (1+\varepsilon_h)(1-\varepsilon_a) & (1+\varepsilon_h)(1+\varepsilon_a) & (1-\varepsilon_a) & (1+\varepsilon_a) \\ (1+\varepsilon_a) & (1-\varepsilon_a) & (1-\varepsilon_h)(1+\varepsilon_a) & (1-\varepsilon_h)(1-\varepsilon_a) \\ (1-\varepsilon_a) & (1+\varepsilon_a) & (1-\varepsilon_h)(1-\varepsilon_a) & (1-\varepsilon_h)(1+\varepsilon_a) \end{bmatrix}. \tag{19}$$

For $\delta\mathbf{B}$, we average over random perturbations to the connectivity matrix $\mathbf{B}_0$. Specifically, we choose $\delta\mathbf{B}$ to be proportional to typical fluctuations of realizations of this SBM:

$$(\delta\mathbf{B})_{ij} \propto \mathcal{N}\big(\mu = 0, \sigma^2 \propto (\mathbf{B}_0)_{ij}(1 - (\mathbf{B}_0)_{ij})\big), \tag{20}$$

then using only the symmetric part $(\delta\mathbf{B} + \delta\mathbf{B}^\top)/2$.[4]

To evaluate the PARE, we construct a symmetric matrix $\mathbf{M}$ that, when evaluating its quadratic form with a vector containing i.i.d. normal entries, results in the PAE of a random perturbation $(1/\gamma_*)$.

We obtain the graph moments up to order $2r = 6$ of the distribution defined by $\mathbf{B}_0$, as well as their derivatives $\mathbf{J}_{\partial\mu/\partial B}$ with respect to the (10) degrees of freedom of $\delta\mathbf{B}$. Using these

---

4. Note that the perturbations are not in terms of $\varepsilon_a$ and $\varepsilon_h$.

moments, we compute the covariance of sample moments up to order $r = 3$ and take its inverse: $\left(\mathbf{\Sigma}^{(\mu)}\right)^{-1}$.

To obtain the desired matrix for moments $\mathbf{M}^{(\mu)}$, we multiply both sides of $\left(\mathbf{\Sigma}^{(\mu)}\right)^{-1}$ with the matrix of partial derivatives, scale by the diagonal matrix $\mathbf{D}_{\sigma_{\delta B}^2}$ of perturbation amplitudes given by Equation 20:

$$\mathbf{M}^{(\mu)} = \left(\mathbf{D}_{\sigma_{\delta B}^2}\right)^{1/2} \left(\mathbf{J}_{\partial \mu / \partial B}\right)^{\top} \left(\mathbf{\Sigma}^{(\mu)}\right)^{-1} \left(\mathbf{J}_{\partial \mu / \partial B}\right) \left(\mathbf{D}_{\sigma_{\delta B}^2}\right)^{1/2}. \tag{21}$$

The matrix for cumulants $\mathbf{M}^{(\kappa)}$ is defined analogously.

As the PARE is a ratio, it is natural to take the log before taking the expectation over the random perturbations. In particular, we can write the $\langle \log \text{PARE} \rangle$ as follows:

$$\begin{aligned}
\left\langle \log \text{PARE} \right\rangle &= \left\langle \log \text{PAE}^{(\kappa)} \right\rangle - \left\langle \log \text{PAE}^{(\mu)} \right\rangle \\
&= \left\langle \log \left( \boldsymbol{\xi}^{\top} \mathbf{M}^{(\kappa)} \boldsymbol{\xi} \right) \right\rangle - \left\langle \log \left( \boldsymbol{\xi}^{\top} \mathbf{M}^{(\mu)} \boldsymbol{\xi} \right) \right\rangle,
\end{aligned}$$

where expectation is taken over $\boldsymbol{\xi}$ having i.i.d. normal entries.

As the distribution for $\boldsymbol{\xi}$ is rotationally symmetric, the entries are i.i.d. normal for any orthogonal basis. In particular, we diagonalize the (positive semidefinite) matrices $\mathbf{M}^{(\mu)}$ and $\mathbf{M}^{(\kappa)}$. Thus, we only need their eigenvalues $\lambda_i$ to compute the expected log PARE:

$$\left\langle \log \text{PARE} \right\rangle = \left\langle \log \sum_i \lambda_i^{(\mu)} \xi_i^2 \right\rangle - \left\langle \log \sum_i \lambda_i^{(\kappa)} \xi_i^2 \right\rangle.$$

At this point, we estimate $\langle \log \text{PARE} \rangle$ via Monte Carlo sampling, resulting in Figure 7.
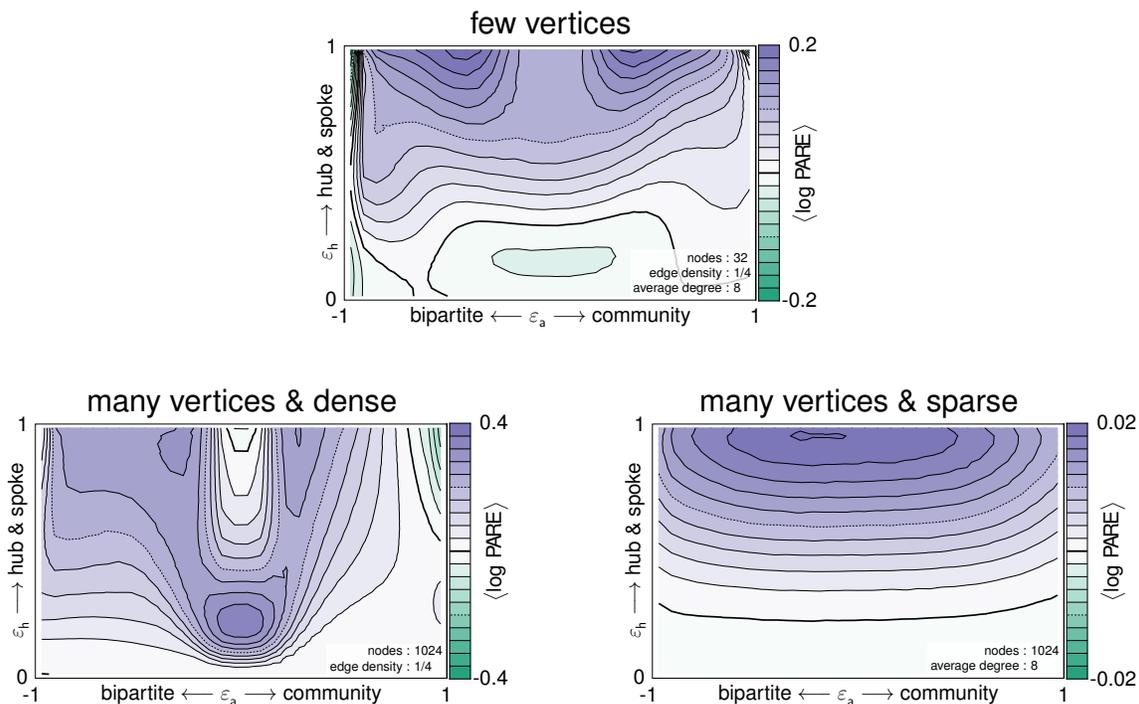
Figure 7: **The test using graph cumulants outperforms that using moments, even in the limit of many observed graphs.**
Here, we compare the asymptotic efficiencies of the two tests in the limit $s \to \infty$. The contours correspond to the $\langle \log \mathrm{PARE} \rangle$ for random perturbations to the SBM defined in Equation 19 (purple indicates that cumulants do better). Note the smaller scale in the sparse regime.

# References

[1] Maryam Aliakbarpour, Amartya Shankha Biswas, Themis Gouleakis, John Peebles, Ronitt Rubinfeld, and Anak Yodpinyanee. Sublinear-time algorithms for counting star subgraphs via edge sampling. *Algorithmica*, 80(2):668–697, 2018.

[2] Uri Alon. Network motifs: theory and experimental approaches. *Nat. Rev. Genet.*, 8 (6):450–461, 2007.

[3] Weihua An. Fitting ergms on big networks. *Social science research*, 59:107–119, 2016.

[4] Dena Asta and Cosma Rohilla Shalizi. Geometric network comparison. *arXiv preprint arXiv:1411.1350*, 2014.

[5] Albert-László Barabási and Réka Albert. Emergence of scaling in random networks. *science*, 286(5439):509–512, 1999.

[6] Christian Borgs, Jennifer T Chayes, László Lovász, Vera T Sós, and Katalin Vesztergombi. Convergent sequences of dense graphs i: Subgraph frequencies, metric properties and testing. *Advances in Mathematics*, 219(6):1801–1851, 2008.

[7] George Casella and Roger L Berger. *Statistical inference*. Cengage Learning, 2021.

[8] Li Chen, Nathaniel Josephs, Lizhen Lin, Jie Zhou, and Eric D Kolaczyk. A spectral-based framework for hypothesis testing in populations of networks. *arXiv preprint arXiv:2011.12416*, 2020.

[9] Yijia Chen, Marc Thurley, and Mark Weyer. Understanding the complexity of induced subgraph isomorphisms. In *International Colloquium on Automata, Languages, and Programming*, pages 587–596. Springer, 2008.

[10] Debarghya Ghoshdastidar and Ulrike Von Luxburg. Practical methods for graph two-sample testing. In *Advances in Neural Information Processing Systems*, pages 3019–3028, 2018.

[11] Debarghya Ghoshdastidar, Maurilio Gutzeit, Alexandra Carpentier, and Ulrike von Luxburg. Two-sample hypothesis testing for inhomogeneous random graphs. *The Annals of Statistics*, 48(4):2208–2229, 2020.

[12] Reid Ginoza and Andrew Mugler. Network motifs come in sets: Correlations in the randomization process. *Phys. Rev. E*, 82(1):011921, 2010.

[13] BV Gnedenko and AN Kolmogorov. *Limit distributions for sums of independent random variables*. Addison-Wesley, 1954.

[14] Lee M. Gunderson and Gecia Bravo-Hermsdorff. Introducing graph cumulants: What is the variance of your social network? *arXiv:2002.03959*, 2020.

[15] Anders Hald. The early history of the cumulants and the gram-charlier series. *Int. Stat. Rev.*, 68(2):137–153, 2000.

[16] Paul W Holland, Kathryn Blackmond Laskey, and Samuel Leinhardt. Stochastic blockmodels: First steps. *Social networks*, 5(2):109–137, 1983.

[17] Mehran Kardar. *Statistical Physics of Particles*. Cambridge Univ. Press., 2007. doi: 10.1017/CBO9780511815898.

[18] Maurice G Kendall et al. The advanced theory of statistics. vols. 1. *The advanced theory of statistics. Vols. 1.*, 1(Ed. 4), 1948.

[19] László Lovász. *Large Networks and Graph Limits*. American Mathematical Soc., 2012.

[20] Prasanta Chandra Mahalanobis. On the generalized distance in statistics. National Institute of Science of India, 1936.

[21] Naoki Masuda, Sadamori Kojaku, and Yukie Sano. Configuration model for correlation matrices preserving the node strength. *Physical Review E*, 98(1):012312, 2018.

[22] PA G Maugis, SC Olhede, CE Priebe, and PJ Wolfe. Testing for equivalence of network distribution using subgraph counts. *J. Comput. Graph. Stat.*, 2020.

[23] Simon Kebede Merid, Daria Goranskaya, and Andrey Alexeyenko. Distinguishing between driver and passenger mutations in individual cancer genomes by network enrichment analysis. *BMC bioinformatics*, 15(1):308, 2014.

[24] Soumendu Sundar Mukherjee, Purnamrita Sarkar, and Lizhen Lin. On clustering network-valued data. *arXiv preprint arXiv:1606.02401*, 2016.

[25] Mark EJ Newman. The structure of scientific collaboration networks. *Proceedings of the national academy of sciences*, 98(2):404–409, 2001.

[26] Jonathan Novak. Three lectures on free probability. *Random matrix theory, interacting particle systems, and integrable systems*, 65(309-383):13, 2014.

[27] Peter Orbanz. Subsampling large graphs and invariance in networks. *arXiv:1710.04217*, 2017.

[28] Guang Ouyang, Dipak K Dey, and Panpan Zhang. Clique-based method for social network clustering. *Journal of Classification*, pages 1–21, 2019.

[29] Jeffrey Pattillo, Nataly Youssef, and Sergiy Butenko. On clique relaxation models in network analysis. *European Journal of Operational Research*, 226(1):9–18, 2013.

[30] Edwin JG Pitman. Notes on non-parametric statistical inference. Technical report, North Carolina State University. Dept. of Statistics, 1949.

[31] CR Rao. Information and accuracy attainable in the estimation of statistical parameters. kotz s & johnson nl (eds.), breakthroughs in statistics volume i: Foundations and basic theory, 235–248, 1945.

[32] Johannes Rauh. The polytope of $k$-star densities. *The Electronic Journal of Combinatorics*, pages P1–4, 2017.

[33] Gian-Carlo Rota and Jianhong Shen. On the combinatorics of cumulants. *J. Combin. Theory A*, 91:283–304, 2000.

[34] Minh Tang, Avanti Athreya, Daniel L Sussman, Vince Lyzinski, Youngser Park, and Carey E Priebe. A semiparametric two-sample hypothesis testing problem for random graphs. *Journal of Computational and Graphical Statistics*, 26(2):344–354, 2017.

[35] Mattia Tantardini, Francesca Ieva, Lucia Tajoli, and Carlo Piccardi. Comparing methods for comparing networks. *Scientific reports*, 9(1):1–19, 2019.

[36] Feng Xia, Haoran Wei, Shuo Yu, Da Zhang, and Bo Xu. A survey of measures for network motifs. *IEEE Access*, 7:106576–106587, 2019.